

## Effects of Magnetite Deposit on Stress Corrosion Cracking of Alloy 600 in All Volatile Treated Water Containing Lead Oxide

Won-Ik Choi<sup>a,b</sup>, Geun Dong Song<sup>a</sup>, Soon-Hyeok Jeon<sup>a</sup>, Sun Jin Kim<sup>b</sup>, Do Haeng Hur<sup>a,\*</sup>

<sup>a</sup> Nuclear Materials Research Division, Korea Atomic Energy Research Institute, 989-111 Daedeok-daero, Yuseong-gu, Daejeon 305-353, Republic of Korea

<sup>b</sup> Division of Materials Science and Engineering, Hanyang University, 222 Wangsimni-ro, Seongdong-gu, Seoul, 04763, Republic of Korea

\*Corresponding author: dhhur@kaeri.re.kr

### 1. Introduction

Extensive laboratory studies for secondary side degradation of Alloy 600 steam generator tubing have been performed and verified that corrosion of Alloy 600 is accelerated in solutions containing various impurities and excused pH conditions [1,2]. However, most of test solutions were too unrealistically strong to appropriately simulate the crevice conditions in operation. It should also be noted that all tubes and heated crevices in operating steam generators are covered with deposits or sludge. The deposits and sludge are porous in nature and consist of mainly magnetite, of which origin is corrosion products released from carbon steel piping by flow accelerated corrosion. This means that real corrosion phenomena occur on the surface of a tube in contact with magnetite. Therefore, the effects of magnetite deposit or sludge should be considered in evaluating the corrosion behavior of steam generator materials.

Recently, we have reported that general corrosion of carbon steel and Ni-based alloys is accelerated by a galvanic effect between the materials and magnetite in various environments [3,4]. Therefore, there is a need to expand our work to the field of stress corrosion cracking phenomena, which have been the major degradation mode of Alloy 600. This paper presents the effect of magnetite on the stress corrosion cracking (SCC) behavior and oxide film property of Alloy 600 in simulated secondary water containing 100 ppm lead oxide (PbO) at 315°C. Lead oxide was chosen as a contaminated impurity in a magnetite-filled crevice, because lead compounds have been known to accelerate stress corrosion cracking of Ni-based alloys [5].

### 2. Experimental Methods

#### 2.1. Preparation of Magnetite Deposited Specimens

Mill-annealed Alloy 600 plate was used as a test material, having an average grain size of about 26.7  $\mu\text{m}$  without intergranular and intragranular chromium carbide precipitations.

To evaluate the effects of magnetite on the SCC behavior of Alloy 600, a SCC specimen should be in contact with magnetite in a test solution. To make this condition, magnetite layer was deposited on the whole

surface of the assembled U-bend SCC specimen except the apex area of 1 mm width. The electrodeposition solution consisted of 2 M NaOH, 0.1 M triethanolamine and 0.043 M  $\text{Fe}_2(\text{SO}_4)_3$ . The electrodeposition of magnetite layer was conducted at an applied potential of  $-1.05 V_{\text{SCE}}$  for 120 min at 80°C.

#### 2.2. SCC Tests

SCC tests were conducted in an all volatile treated (AVT) solution containing 100 ppm PbO at 315°C. Before heating the autoclave, the test solution was deaerated by blowing high purity argon gas with a flow rate of 300 ml/min in the closed autoclave for 4 hrs. The autoclave operation was stopped to examine the U-bend specimens after a period of 350 hr, 650 hr, and 1000 hr, respectively. The test solution was refreshed and deaerated whenever the autoclave was closed after inspection of the test specimens.

#### 2.3. Crack Examination and Oxide Film Analysis

The U-bend specimens were destructively examined to measure the depth and morphology of stress corrosion cracks. TEM specimens including the outer surfaces and cracks were prepared using the focused ion beam. TEM imaging and elemental compositions of oxides were then analyzed using an energy dispersive X-ray spectroscopy (EDS)

### 3. Results and Discussion

Fig. 1 shows the typical stress corrosion cracks in Alloy 600 uncoupled and coupled with magnetite, which were tested for 650 h. It should be noted that the deepest cracks was always observed at the apex of the uncoupled specimens, whereas the maximum depth of the cracks was always observed near the interface between the deposited magnetite and the exposed Alloy 600. All cracks were initiated and propagated along the grain boundaries.

Fig. 2 shows the evolution of the maximum crack depth with testing time, which was measured from 2 or 3 U-bend specimens for each condition. The magnetite deposited specimens always revealed a much deeper crack depth than the uncoupled reference specimens at a given test time.

Here, we can use two ways to define the crack growth rate (CGR). First, the CGR can be simply defined as an average value when dividing the maximum crack depth by a given test time, without considering the incubation time of a crack. Then, the CGR values are calculated to be approximately  $0.45 \mu\text{m/h}$  for the uncoupled specimens and  $0.80 \mu\text{m/h}$  for the coupled specimens. This result indicates that the CGR of the coupled specimen is faster approximately 56% than that of the uncoupled specimen. Secondly, the CGR can be estimated by the slope of the crack depth versus test time axis. In this case, the CGRs yielded from the best-fitted data were very similar to each other:  $0.73 \mu\text{m/h}$  for the uncoupled specimens and  $0.79 \mu\text{m/h}$  for the uncoupled specimens. From the best-fitting in Fig. 2, the incubation time can also be estimated: 70 h for the coupled specimens and 200 h for the uncoupled specimens. This indicates that the incubation time to cracking of Alloy 600 decreased to a third by the coupling with magnetite in this test condition. Once cracks initiate, however, the cracks grow with the same CGR regardless of the presence of magnetite. Similarly, based on the collected data from the literature [5, 6], Wright and Mizrai showed that the CGR of Alloy 600MA in AVT water containing PbO at  $320^\circ\text{C}$  was approximately  $0.2 \mu\text{m/h}$ , independent of the PbO concentration from 1 to 2,000 ppm [7].

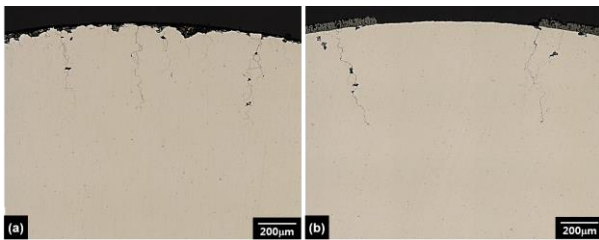


Fig. 1. Stress corrosion cracks in Alloy 600 after a 650-hr test: (a) uncoupled, and (b) coupled with magnetite.

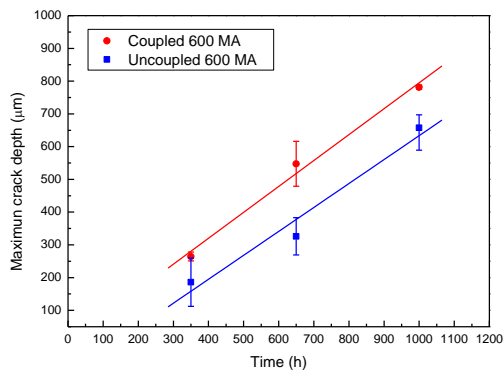


Fig. 2. Evolution of the maximum crack depth of Alloy 600 with testing time in AVT water with 100 ppm PbO at  $315^\circ\text{C}$ .

Fig. 3 shows the SEM images on the outer alloy surfaces near the apex region of the U-bend specimens

after a 650-hr SCC test. Polyhedral oxides were formed on the uncoupled specimen, whereas porous, broken glass-shaped oxides were observed on the coupled specimen. These obviously different features of surface oxides could be attributed to the SCC behaviors shown in Fig. 2. Because TEM-EDS analysis of the oxides is ongoing, a detailed explanation and discussion will be given in the autumn meeting of this conference.

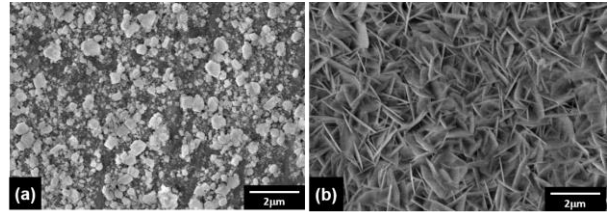


Fig. 3. SEM images on the outer alloy surface near the apex region of the U-bend specimens after a 650-hr test: (a) uncoupled, and (b) coupled with magnetite.

#### 4. Conclusions

Stress corrosion tests for Alloy 600 were conducted to investigate the effects of magnetite in an all volatile treated water containing 100 ppm PbO, simulating the corrosion of Alloy 600 beneath porous magnetite deposits in a SG. The tentative conclusions can be drawn as follows.

1) Alloy 600 specimens coupled with magnetite produced stress corrosion cracks approximately 56% deeper than uncouple specimens at a given test time in this test condition.

2) The galvanic coupling with magnetite decreased the incubation time to cracking of Alloy 600 to a third, without the change of the crack growth rate.

3) Polyhedral oxides were formed on the uncoupled specimen, whereas porous, broken glass-shaped oxides were observed on the coupled specimen. These obviously different features of surface oxides could be attributed to the SCC behaviors.

#### ACKNOWLEDGEMENTS

This work was supported by the National Research Foundation of Korea (NRF) grant funded by the Korea government (MSIP) (2017M2A8A4015159).

#### REFERENCES

- [1] I.J. Yang, Effect of Sulphate and Chloride Ions on the Crevice Chemistry and Stress Corrosion Cracking of Alloy 600 in High Temperature Aqueous Solutions, *Corrosion Science*, Vol. 33, No. 1, pp. 25-37, 1992.
- [2] J. R. Crum, Stress Corrosion Cracking Testing of Inconel Alloys 600 and 690 under High-Temperature Caustic Conditions, *Corrosion*, Vol. 42, No. 6, pp. 368-372, 1986.
- [3] S.H. Jeon, G.D. Song, D.H. Hur, Corrosion Behavior of Alloy 600 Coupled with Electrodeposited Magnetite in

Simulated Secondary Water of PWRs, *Materials Transactions*, Vol. 56, No. 12, pp. 2078-2083, 2015.

[4] S.H. Jeon, G.D. Song, D.H. Hur, Galvanic Corrosion between Alloy 690 and Magnetite in Alkaline Aqueous Solutions, *Metals*, Vol. 5, No. 4, pp. 2372-2382, 2015.

[5] H. Takamatsu, B.P. Miglin, P.A. Sherburne, K. Aoki, Study on Lead-Induce Stress Corrosion Cracking of Steam Generator Tubing under AVT Water Chemistry Conditions, *Proceedings of Eighth International Symposium on Environmental Degradation of Materials in Nuclear Power System – Water Reactors*, Amelia Island, FL, TMS, pp. 216-223, 1997.

[6] M.L. Castano-Martin, D. Gomez-Briceno, F. Hernandez-Arroyo, Influence of Lead Contamination on Stress Corrosion Resistance of Nickel Alloys, *Proceedings of Sixth International Symposium on Environmental Degradation of Materials in Nuclear Power Systems – Water Reactors*, San Diego, CA, TMS, pp. 189-196, 1993

[7] Wright, Mizrai, Lead-Induced SCC Propagation Rates in Alloy 600, *Proceedings of Ninth International Symposium on Environmental Degradation of Materials in Nuclear Power Systems – Water Reactors*, Newport Beach, CA, TMS, pp. 657-664, 1999